

# TWO-STAGE TLM MODELLING APPROACH FOR MORE EFFICIENT ANALYSIS OF VEHICLE ANTENNA INSTALLATIONS

A.R. Ruddle

MIRA Limited, UK (alastair.ruddle@mira.co.uk)

**Keywords:** equivalent surface source, TLM, vehicle.

## Abstract

Modelling the installed performance of vehicle-mounted antennas remains a significant computational challenge. A two-stage approach, based on the use of an equivalent surface source, avoids the need to include the antenna geometry in the installation model. This approximation can very significantly reduce memory requirements and computing time. Numerical experiments suggest that this can provide a more efficient approach for installations based on simple structures, but that greater caution may be required for applications involving more complex geometries, such as passenger cars.

## 1 Introduction

Vehicle geometry can have a significant impact on the installed performance of antennas that are mounted on the structure, which may have implications for intended system performance. Transmissions in the vehicle environment also have potential safety implications, in terms of electromagnetic compatibility and occupant field exposure. Consequently, early knowledge of the properties of vehicle antenna installations is increasingly important to support cost effective development processes.

Although whole-vehicle electromagnetic modelling is now feasible, the computational resources required to address the frequencies and physical structures of interest remain a major challenge. Time-domain methods based on structured meshing, such as TLM and FDTD, are attractive for such applications because their memory usage is relatively frugal and a single simulation can provide a broadband response. The total number of cells and the size of the smallest cells are the main influences for the computational requirements. Thus, it is highly desirable to avoid the very small cell sizes that would be needed to accommodate intricate antenna structures in whole-vehicle models.

## 2 Two-stage approximation

The commercial TLM code “Microstripes” [2] provides facilities for exciting a model using an equivalent surface source. This source model can be obtained from the field distribution over a surface of the same physical extent in the

near-field of a separate and more detailed simulation of the antenna structure. Data obtained for a regular series of frequencies is then used to generate a set of corresponding time series that are used to excite the equivalent surface cells in the approximate models.

The more finely resolved distribution from the detailed antenna model must be averaged over the larger cells of the source surface in the installation model. Thus, the errors in this two-stage approach are likely to depend on features such as the disparity between the cell sizes of the approximate and detailed models, the sampling frequency increment, the proximity of the equivalent surface to the antenna, and the nature of the parameters of interest. The two-stage approach requires at least one additional model to be run (perhaps more for multi-band devices), but if the errors due to the approximation can be tolerated the anticipated savings in terms of memory and run-time for whole-vehicle simulations would significantly exceed the cost of the additional models.

For use in automotive applications, the installation must be such that a rectangular equivalent surface that contains the antenna can also be matched to the model of the structure that supports the antenna. A further limitation is that it may not always be possible to achieve an adequate representation of the influence of nearby structures on the antenna in the separated model. These issues could be significant for complex regions such as a wheel arch, but perhaps less so for antennas located on large body panels.

## 3 Antenna and discretization schemes

The antenna used as a test case for these investigations (see Fig. 1) is a dual-band planer inverted-F type structure [3] that has previously been studied installed on a passenger car [1].

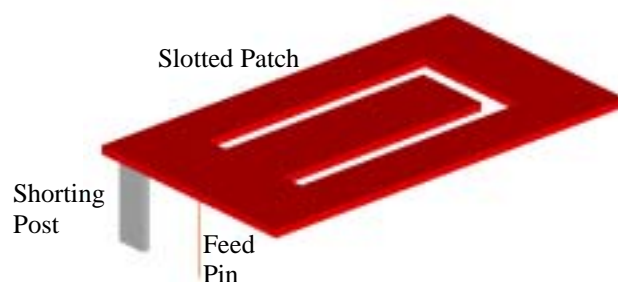


Fig. 1: Antenna structure used for investigation.

The antenna dimensions were chosen (based on [3]) in order to provide resonant frequencies that would approximate those used for mobile telephone transmissions. However, there was no attempt to optimise the design in any detail, as it was only intended for numerical experimentation purposes.

The patch was 5 cm long, 3 cm wide and mounted 1 cm above the ground plane. The detailed model used to generate the equivalent sources for the approximate models was based on a 1 mm cubic mesh over the antenna elements and their immediate vicinity. An intermediate layer of three 3 mm cells then surrounded this core region, beyond which a 1.5 cm mesh was applied.

The same meshing strategy was also applied in the detailed models for the antenna when mounted on other structures, which were used to assess the results from the approximate models. The approximate models all used a 15 mm cubic mesh throughout, with the size and location of equivalent surface source matched that of the antenna and associated output region in the detailed models.

#### 4 Ideal conditions

Electric field data was obtained in the vicinity of the antenna over an infinite ground plane for a nearby point and a more distant point (at 17 cm and 124 cm, respectively). The results from the approximate models are compared with those from the detailed model in Figs. 2-3 for frequencies around the first resonance, while Figs. 3-4 show corresponding results for the second resonance. Data for a sequence of 40 frequencies was used to derive the equivalent surface excitation in both bands.

It was expected that the impact of mapping the detailed equivalent surface source onto the coarser mesh of the approximate model would be smaller at greater distances. This appears to be the case around the first resonance, but for the second resonance the deviation is greater for the more distant point. Nonetheless, these results suggest that the approximation works very well under ideal conditions. The largest error was 2.5%, for the more distant point at the second resonance (see Fig. 5).

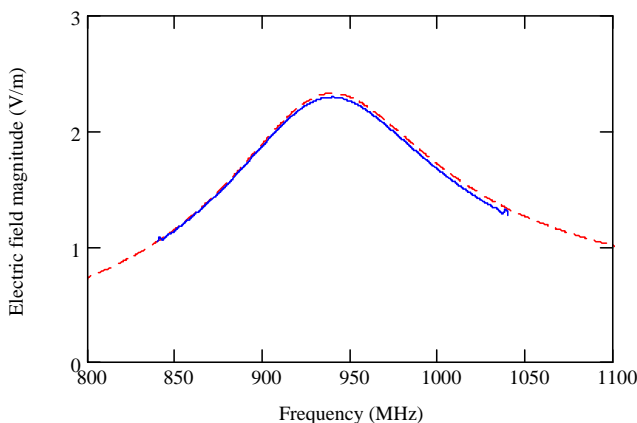


Fig. 2: Electric field at 1<sup>st</sup> resonance for nearby point: detailed (dashed) and approximate (solid) models.

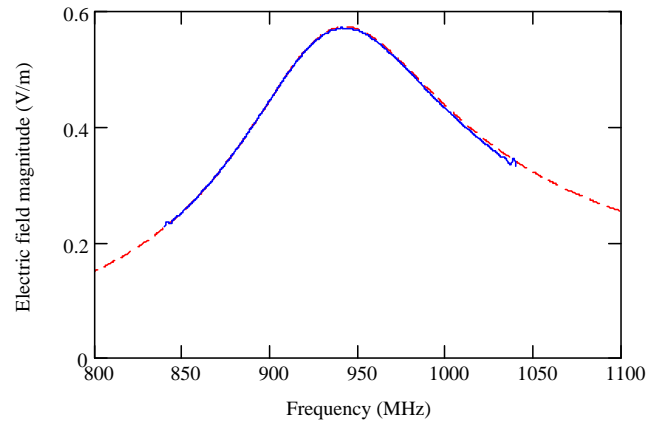


Fig. 3: Electric field at 1<sup>st</sup> resonance for more distant point: detailed (dashed) and approximate (solid) models.

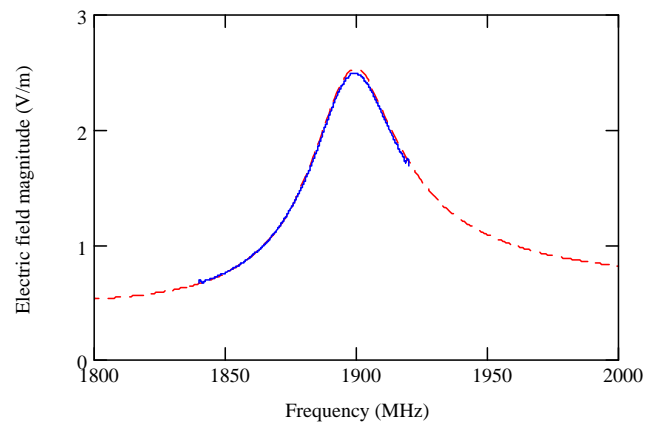


Fig. 4: Electric field at 2<sup>nd</sup> resonance for nearby point: detailed (dashed) and approximate (solid) models.

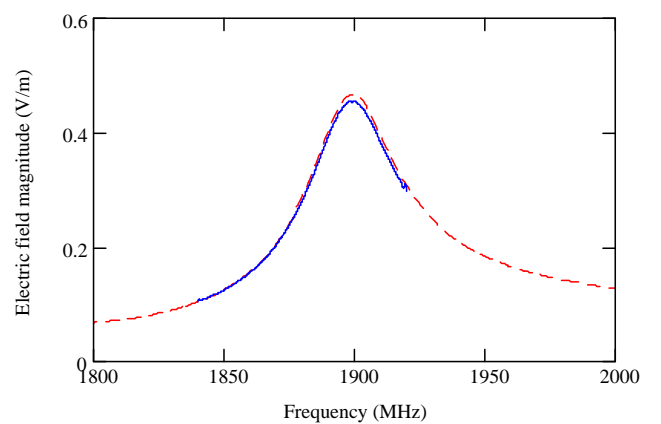


Fig. 5: Electric field at 2<sup>nd</sup> resonance for more distant point: detailed (dashed) and approximate (solid) models.

The radiation patterns obtained from the approximate models at resonance were essentially identical to those of the detailed models. The errors in the maximum gain values were 0.86% at first resonance and 1.15% at the second resonance.

In this example the approximate models required 26 Mbytes and ran for 2 minutes, while the detailed model required around 150 Mbytes and 60 minutes.

## 5 Antenna on conducting block

As an example of a very simple installation, the antenna was placed on a large conducting block, with the more distant field output point located below the edge of the block (see Fig. 6). The nearby point was located at 23 cm from the antenna, while the more distant point was at 84 cm distance.

The block was 79.5 cm long, 90 cm wide and 54 cm deep. The antenna axis was aligned with the axis of the block, but displaced towards one end. The computational volume was identical in the detailed and approximate models in order to ensure that any boundary reflections would be identical.

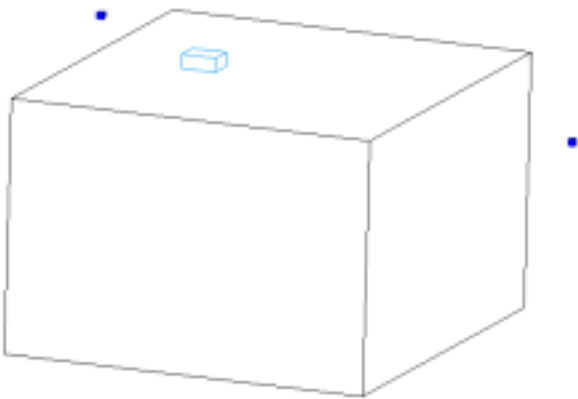


Fig. 6: Equivalent surface source on conducting block (shaded blocks indicate field output points).

The detailed model required 1.1 GBytes and took 4 hours to run, while the approximate models required only 0.45 GBytes and 2.5 hours computing time. The detailed model of the ideal antenna used to derive the equivalent source data required only 80 Mbytes and 10 minutes computing time.

### Block - first resonance

The electric field outputs (see Figs. 7-8) show larger errors than the ideal case, particularly for the more distant point. However, the amplitude error in Fig. 8 is only 7.8% at resonance.

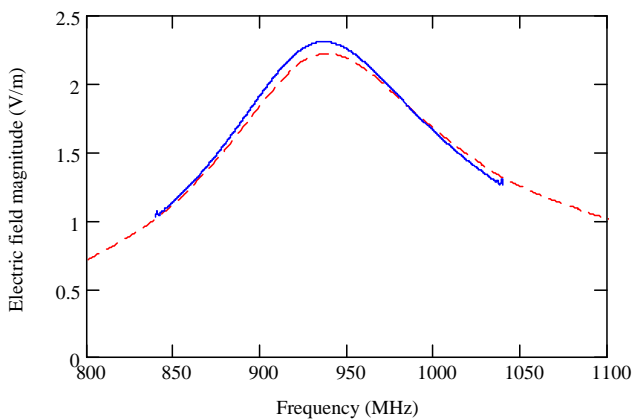


Fig. 7: Electric field at 1<sup>st</sup> resonance for nearby point: detailed (dashed) and approximate (solid) models.

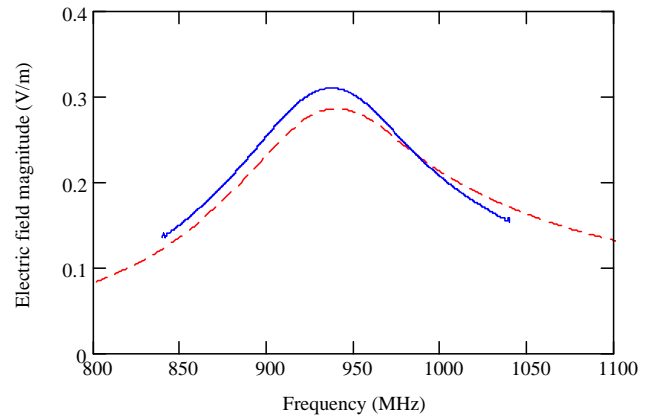


Fig. 8: Electric field at 1<sup>st</sup> resonance for more distant point: detailed (dashed) and approximate (solid) models.

The projected far-field radiation patterns in the azimuth plane are slightly asymmetric (see Fig. 9), perhaps due to the asymmetry of the antenna structure. The underlying topology of the patterns is very similar, although there are differences of up to 10 dB in some directions. However, the elevation plane patterns (see Fig. 10) are very similar except in the case of the very deep null that occurs at  $-164^\circ$  in the detailed model.

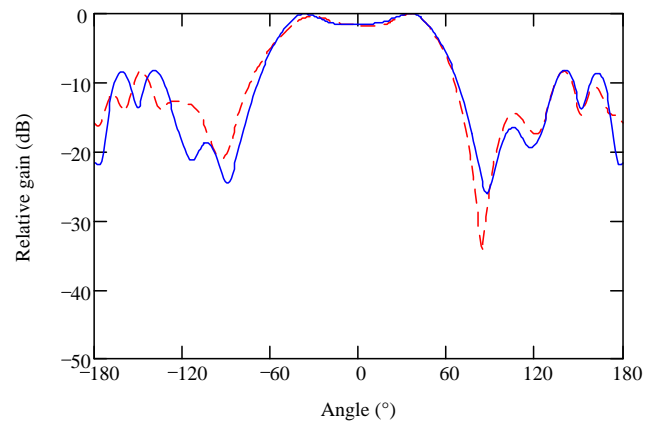


Fig. 9: Azimuth plane pattern for block at 1<sup>st</sup> resonance: detailed (dashed) and approximate (solid) models.

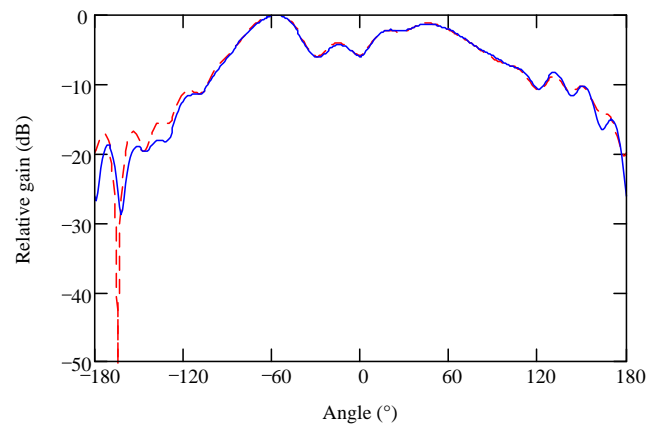


Fig. 10: Elevation plane pattern for block at 1<sup>st</sup> resonance: detailed (dashed) and approximate (solid) models.

### Block - second resonance

Results for the electric field outputs are shown in Figs. 11-12, and the largest error in the electric field results is again for the more distant point at second resonance (reaching 9.5% in this case). The azimuth patterns are very similar and almost omnidirectional in this case (see Fig. 13), but the correlation between the elevation plane patterns (see Fig. 14) is poorer.

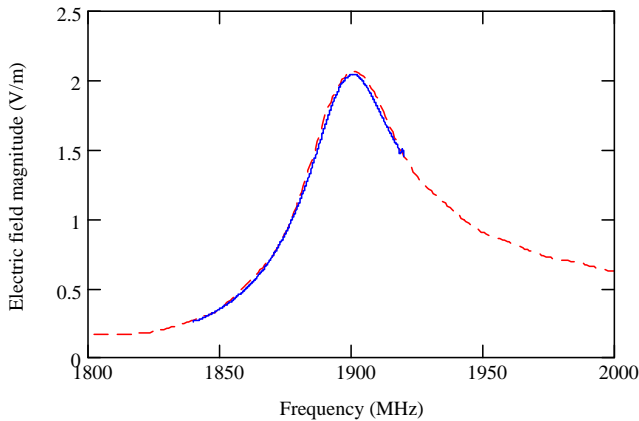


Fig. 11: Electric field at 2<sup>nd</sup> resonance for nearby point: detailed (dashed) and approximate (solid) models.

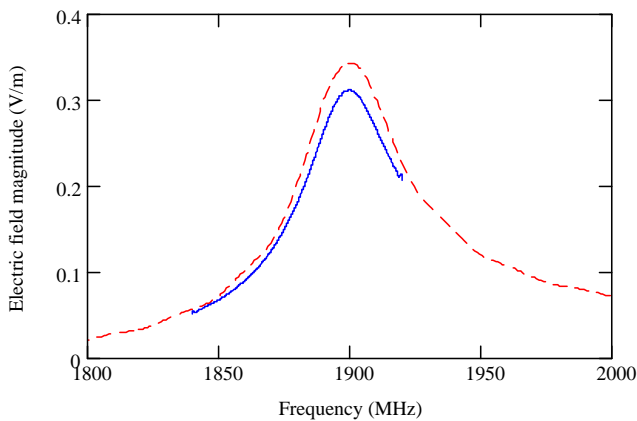


Fig. 12: Electric field at 2<sup>nd</sup> resonance for more distant point: detailed (dashed) and approximate (solid) models.

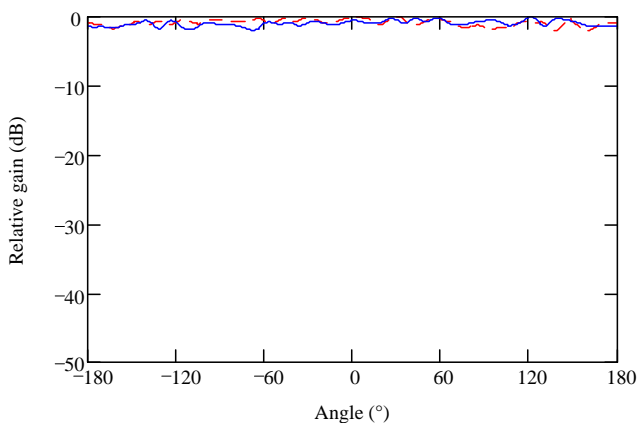


Fig. 13: Azimuth plane pattern for block at 2<sup>nd</sup> resonance: detailed (dashed) and approximate (solid) models.

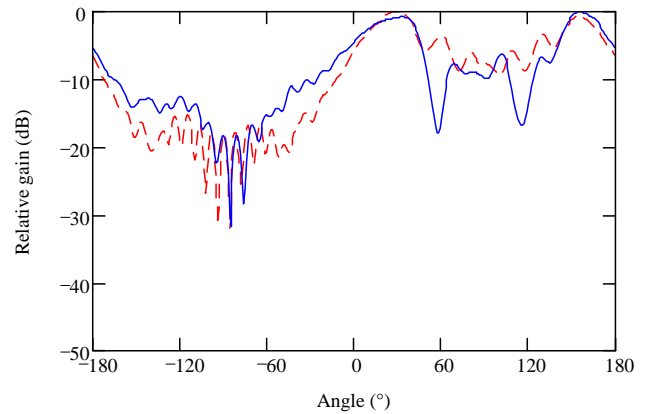


Fig. 14: Elevation plane pattern for block at 2<sup>nd</sup> resonance: detailed (dashed) and approximate (solid) models.

## 6 Passenger car installation

In order to investigate a vehicle installation of more realistic complexity, the antenna was located on the boot lid of a passenger car model, and aligned with the longitudinal axis (see Fig. 15). For the purposes of this study the content of the car model was limited to the major metallic parts only.

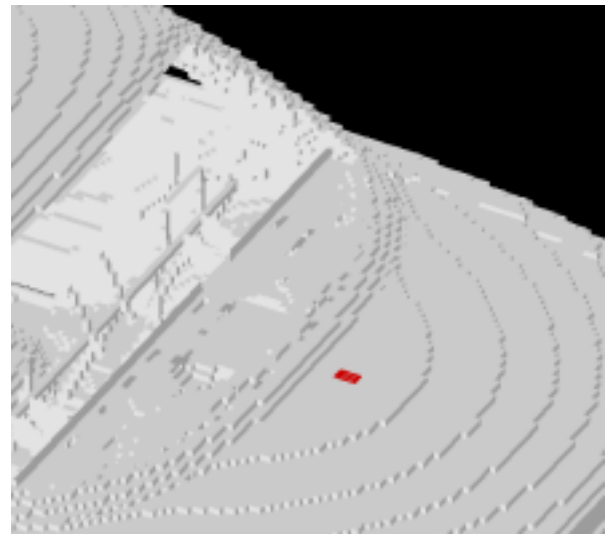


Fig. 15: Rear view of car model, indicating location of antenna structure on boot lid.

In this example the nearby point is towards the rear of the car, at a similar distance to that used in the simpler system, while the more distant point is in the vicinity of the front seats.

The approximate models for the car-mounted installation required 1.8 Gbytes and ran for 6.5 hours. However, the detailed model required 3.3 GBytes and 113 hours computing.

### Car - first resonance

The results obtained in this case show larger errors than for the two simple cases. Although the external field for the first resonance is reasonably close (see Fig. 14), the correlation for the internal field response is rather poor (see Fig. 15).

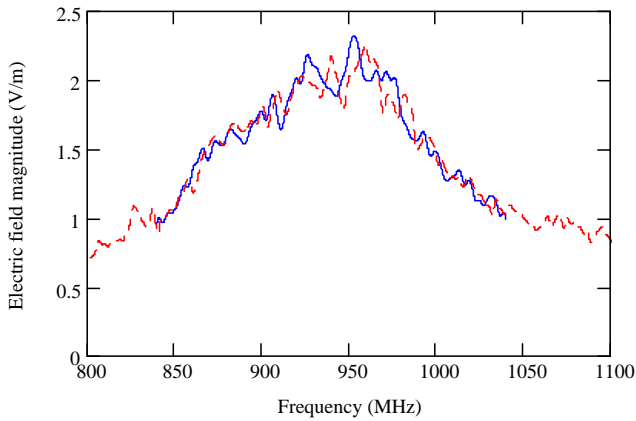


Fig. 16: Electric field at 1<sup>st</sup> resonance for nearby point: detailed (dashed) and approximate (solid) models.

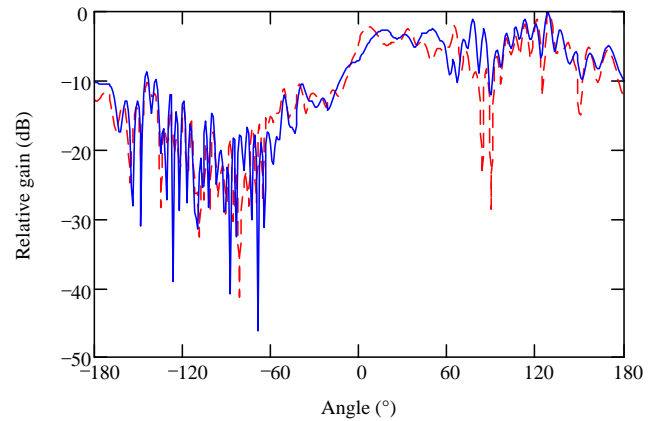


Fig. 19: Elevation plane pattern for car at 1<sup>st</sup> resonance: detailed (dashed) and approximate (solid) models.

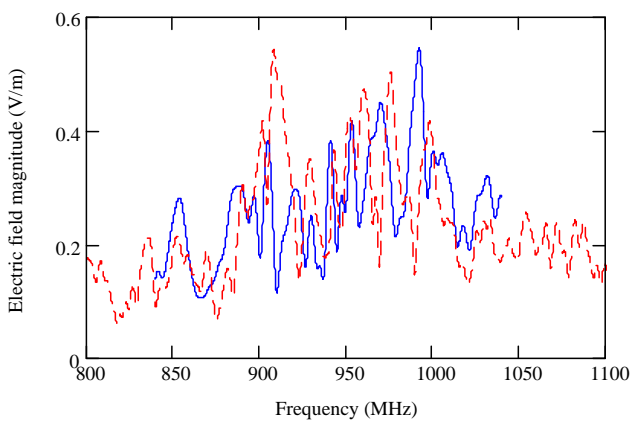


Fig. 17: Electric field at 1<sup>st</sup> resonance for more distant point: detailed (dashed) and approximate (solid) models.

The radiation patterns from the detailed and approximate models generally show similar topology. The azimuthal patterns are fairly similar (see Fig. 18), but there are some significant differences in the details for the elevation plane pattern (see Fig. 19). Asymmetries in the internal geometry of the car may also contribute to the asymmetry in the azimuthal radiation pattern.

### Car - second resonance

The detailed model for car installation indicates a marked upward shift in the frequency of the second resonance, so radiation patterns are not compared in this case. Nonetheless, the field levels and shapes are similar for the external and internal points (see Fig. 20-21).

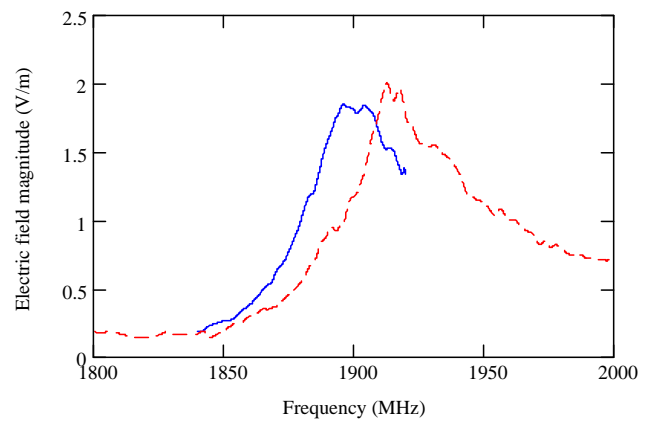


Fig. 20: Electric field at 2<sup>nd</sup> resonance for nearby point: detailed (dashed) and approximate (solid) models.

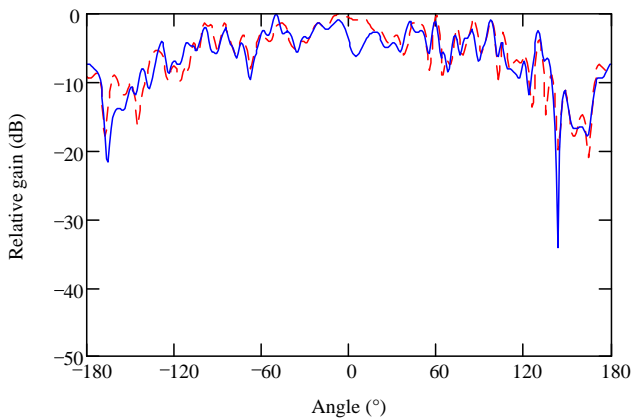


Fig. 18: Azimuth plane pattern for car at 1<sup>st</sup> resonance: detailed (dashed) and approximate (solid) models.

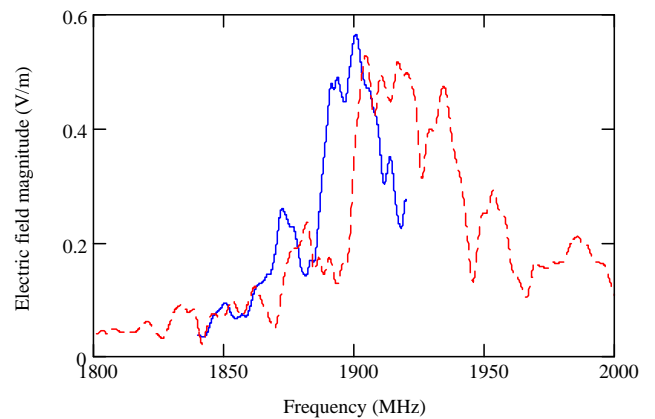


Fig. 21: Electric field at 2<sup>nd</sup> resonance for more distant point: detailed (dashed) and approximate (solid) models.

## 7 Input match

The return loss responses obtained from the detailed models for the three test configurations are illustrated in Fig. 22 for the first resonance, while Fig. 23 shows results for the second resonance. These results demonstrate the impact of the installation on the impedance properties of the antenna, and show that the structure of the car produces a marked shift in the frequency of the second resonance.

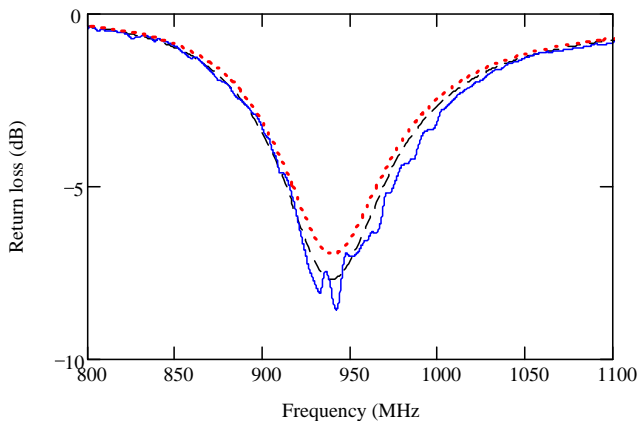


Fig. 22: Return loss at 1<sup>st</sup> resonance: ideal antenna (dotted), antenna on block (dashed) and on car (solid).

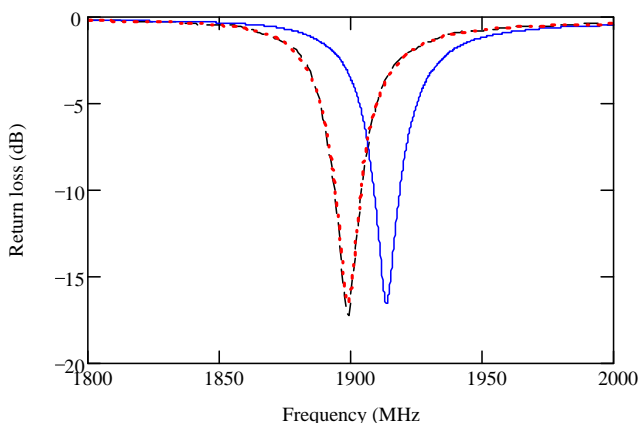


Fig. 23: Return loss at 2<sup>nd</sup> resonance: ideal antenna (dotted), antenna on block (dashed) and on car (solid).

## 8 Conclusions

The two-stage method works very well for the antenna under ideal conditions, with no nearby conductors present. For the block-mounted antenna the errors are greater than for the ideal environment, but are probably sufficiently good to be of practical use in many applications.

Although it was anticipated that there would be a number of practical limitations to the use of the two-stage approach for modelling passenger cars, the installation studied here was expected to provide a relatively benign test-case. For this configuration, however, the approximation method was found to be less successful than for the case with the antenna mounted on the simple block structure.

For the car, the far-field patterns are fairly representative for the first resonance, and so might be useful for initial investigations of antenna placement options. However, the quality of the internal field results does not give confidence that it could be successfully used in human exposure or EMC investigations. Adding a simplified representation of the missing geometry (to emulate scattering from the antenna) had no discernible impact on the results. For the second resonance the significant frequency shift is a major problem, which could make the approximation of limited value if this phenomenon cannot be identified without recourse to a whole-vehicle model. Further work will investigate whether this effect can be predicted from a more representative (but still small) detailed model, and evaluate the performance of the two-stage approach in other installation configurations.

The approximate models for the car installation ran for some 6.5 hours and required 1.8 Gbytes, while the detailed model required 3.3 Gbytes and 113 hours computing. Thus, the two-stage approach provided results for the vicinity of the two resonances overnight, while the detailed model took 5 days to run (although this model also provides results at a much wider range of frequencies). These very significant savings in memory requirements and computing time could offset the limitations of the approximation for some applications.

The results suggest that the two-stage approach could perhaps more readily deliver the anticipated benefits in applications where the vehicle geometry is of a simpler and more enclosed nature than a passenger car. Possible examples could include aircraft and trains, as well as industrial and fighting vehicles.

## Acknowledgements

The work outlined above was partly supported by SEFERE, a collaborative research project funded by the UK Department of Trade and Industry (Technology Programme reference TP/3/DSM/6/I/15266). The consortium includes MIRA Ltd (coordinator), ARUP Communications, BAE Systems Ltd, Harada Industries Europe Ltd, Jaguar Cars, National Policing Improvements Agency, Sheffield University and Volvo Car Corporation (Sweden). Further information can be found on the project website (<http://www.sefere.org>).

## References

- [1] P. Ankarson, J. Carlsson and Y. Liu, "Numerical study of a PIFA mounted on a car compared to measurements", *Proc. IEEE 2005 EMC Symposium*, Chicago, USA, pp. 878-882 (2005).
- [2] D.P. Johns, R. Scaramuzza and A.J. Wlodarczyk, "Micro-Stripes – microwave design tool based on 3D-TLM", *Proc. 1st International Workshop on Transmission Line Matrix (TLM) Modeling – Theory and Applications*, Victoria, Canada, pp.169-177 (1995).
- [3] P. Salonen, M. Keskilammi and M. Kivikoski, "Single-feed dual-band planar inverted-F antenna with U-shaped slot", *IEEE Trans. Antennas and Propagation*, **48**(8), p.1262-1264 (2000).